

Electronic Supplementary Information

Iron-cobalt Bimetal Oxide Nanorods as Efficient and Robust Water Oxidation Catalyst

Xichen Zhou,^a Jingwei Huang,^a Fuming Zhang,^a Yukun Zhao,^a Yan Zhang,^a Yong Ding^{a,b,*}

^a State Key Laboratory of Applied Organic Chemistry, Key Laboratory of Nonferrous Metals Chemistry and Resources Utilization of Gansu Province, College of Chemistry and Chemical Engineering, Lanzhou University, Lanzhou 730000, China

^b State Key Laboratory of Rare Earth Resource Utilization Changchun Institute of Applied Chemistry, Chinese Academy of Sciences, Changchun 130022, P.R. China

E-mail: dingyong1@lzu.edu.cn

Experiment section

Materials.

All chemicals of analytical grade were used in the experiment directly without further purification. Purified water (18.2 M Ω cm) used for preparing solutions was made by Molecular Lab Water Purifier.

Synthesis of Mn_{1.1}Co_{1.9}O₄ sample.

In the course of synthesis, poly(ethylene oxide)–poly(propylene oxide)–poly(ethylene oxide) (P123, 1.00 g) and oxalic acid (H₂C₂O₄ 2.80 g) were totally dissolved in a mixed solution of ethanol (25 mL) and PEG (Mw = 200, 100 mL) with magnetic stirring. Later, 0.5 M of MnSO₄·H₂O (5 mL) and 0.5 M of Co(NO₃)₂·6H₂O (10 mL) were both added into the above solution. Then, the solution was stirred for 15 min to form the precipitates which were collected by centrifugation and washed with deionized water as well as absolute ethanol for several times. Whereafter, the light red precipitates were dried in air at 60°C for 6 h. Finally, through an annealed process at 400°C for 3 h, Mn_{1.1}Co_{1.9}O₄ sample was obtained.

Synthesis of Fe_{1.1}Co_{1.9}O₄ sample.

The synthesis method of Fe_{1.1}Co_{1.9}O₄ sample is as same as the Mn_{1.1}Co_{1.9}O₄ sample, except that FeSO₄·7H₂O was used to replace MnSO₄·H₂O. Differently, orange precipitates formed in the mixed solution.

Synthesis of Co₃O₄ sample.

The synthesis process of Co₃O₄ sample is similar to the Mn_{1.1}Co_{1.9}O₄ sample. However, only 0.5 M Co(NO₃)₂·6H₂O (15 mL), as the sole source of metal, was added into the former solution. Then, wine red precipitates were obtained.

Synthesis of Fe₂O₃ sample.

The synthesis method of Fe₂O₃ sample is same as the Fe_{1.1}Co_{1.9}O₄ sample. Except, only 0.5 M FeSO₄·7H₂O (15 mL), as the sole source of metal, was added into the previous solution.

Synthesis of Mn₂O₃ sample.

The synthesis method of Mn₂O₃ sample is same as the Mn_{1.1}Co_{1.9}O₄ sample. But, just 0.5 M MnSO₄·H₂O (15 mL) was added into the former solution.

Synthesis of Fe₃O₄ sample.

Fe₃O₄ sample was synthesized according to the reported literature.^{s1} FeCl₃·6H₂O (2.0 mmol, 0.54 g) and sodium citrate (4.0 mmol, 1.176 g) were dissolved in 40 mL aqueous solution, which was added polyacrylamide (0.30 g) and ammonia (25%, 0.50 mL), with vigorous magnetic stirring at room temperature. The mixtures were then stirred vigorously for 30 min and moved into a 100 mL stainless-steel autoclave with Teflon-lined later. The hermetic tank was then heated to and held with a temperature of 200 °C for 12 h. This solid product was gathered by centrifugation and washed with deionized water as well as absolute ethanol for several times. Finally, the powder was dried in a drying oven with 100 °C for 10 h.

Catalysts characterizations

A Rigaku D/MAX 2400 diffractometer (Japan) was used to obtain the Powder X-ray diffraction (PXRD) data with a Cu K α radiation ($\lambda = 1.5418 \text{ \AA}$) working at 60 mA and 40 kV. X-ray photoelectron spectra (XPS) were surveyed by ESCALAB250xi instrument with X-ray

monochromatisation. C 1s peak (284.8 eV) from residual carbon was used to correct the binding energy of other elements. Field emission scanning electron microscopy (FE-SEM) images of samples were undertaken on a Hitachi S-4800 operating at an scanning voltage of 5.0 kV. Transmission electron microscopy (TEM), high resolution TEM (HRTEM) and selected area electron diffraction (SAED) data were collected by a TecnaiG²F30 instrument. Infrared spectra were measured by a Bruker VERTEX 70v FT-IR spectrometer with 2-4 wt% samples in KBr pellets. TU-1810 spectrophotometer fabricated by Beijing Purkinje General Instrument Co. Ltd. equipped with a photomultiplier tube detector was employed to obtain the UV-Vis absorption spectra.

Photocatalytic water oxidation

Water oxidation experiments were performed according to the well-established [Ru(bpy)₃]²⁺ - S₂O₈²⁻ protocol. Initially, a 10 mL solution was prepared by mixing catalysts (0.5 g L⁻¹), [Ru(bpy)₃]Cl₂ (1.0 mM) and Na₂S₂O₈ (5.0 mM) in a borate buffer solution (pH 9.0) in the dark. Then, the above solution was deaerated with Ar gas to remove O₂ in both liquid phase (10 mL) and head space of vial (15.8 mL) for 15 min in a special flask sealed by a rubber plug. Next, the reactor was illuminated with an LED light source (15.8 mW, beam diameter = 2 cm) with a cut off glass filter ($\lambda \geq 420$ nm) at room temperature. After each detecting interval, 100 μ L of Ar gas was pushed into the special flask and then same 100 μ L of the gas in the head space of the vial was taken with a SGE gas-tight syringe and determined by gas chromatography (GC) equipped with 5 Å molecular sieves and thermal conductivity detector (TCD). The entire amount of generated O₂ was calculated by the concentration of O₂ that dispersed in the headspace gas. Nanosecond transient absorption measurements were performed on an Edinburgh Instruments LP920-KS laser flash photolysis spectrometer, using an OPO laser source (OPOTEK Vibrant). Transient detection was obtained using a photomultiplier-oscilloscope combination (Hamamatsu R928P, Tektronix TDS3012C). Kinetics of bleach recovery conditions: Excitation wavelength = 445 nm, analysis wavelength = 450 nm.

Electrocatalytic water oxidation

The electrochemistry experiments were recorded on a CHI660D electrochemical analyzer connected with a standard three-electrode system using a glassy carbon as the working electrode (GCE, 3 mm in diameter) with Ag/AgCl (3.5 M KCl, $E_{\text{NHE}} = E_{\text{Ag/AgCl}} + 0.208$, $E_{\text{RHE}} =$

$E_{\text{Ag/AgCl}} + 0.208 + \text{pH} \times 0.059$) and Pt wire electrode as reference and counter electrodes, respectively. The working electrode was pasted with 0.01 mg catalyst executed by dispersing 1 mg catalyst powder in 400 μL ethanol and then 4 μL of solution dropped onto the glassy carbon electrode slowly. (0.04 mg catalyst was loaded on GEC for Mott-Schottky measurement) Next, 2.5 μL of 0.5 wt % nafion was cast on the dried catalyst film to improve the physical stability of the as-prepared membrane electrode. LSVs plots were acquired in 1 M potassium hydroxide (pH 13.6) solution from 0.3 to 0.7 V vs. Ag/AgCl with a scanning rate of 10 mV s^{-1} . Cyclic voltammetry (CV) was recorded at room temperature with a scanning rate of 100 mV s^{-1} . Electrochemical impedance spectroscopy (EIS) was performed at 1.56 V vs RHE by applying an AC voltage of 5 mV amplitude and frequency range from 100,000 to 0.1 Hz in 1 M potassium hydroxide solution. Tafel slopes were obtained from the LSVs plots through mapping the overpotential η vs $\log(J)$. Mott-Schottky analysis was processed through using a measured voltage from 0.2 V to 1.0 V vs. Ag/AgCl with an AC voltage of 10 mV amplitude and frequency of 5 KHz by a voltage amplification of 10 mV in a 80mM borate buffer (pH 9.0).

Calculation methods

The conversion of electrode potential under different standards

$$E_{\text{NHE}} = E_{\text{Ag/AgCl}} + 0.208$$

$$E_{\text{RHE}} = E_{\text{Ag/AgCl}} + 0.208 + \text{pH} \times 0.059$$

Apparent quantum yield calculation

Initial O_2 formation rate: 0.074 $\mu\text{mol s}^{-1}$ for $\text{Fe}_{1.1}\text{Co}_{1.9}\text{O}_4$; 0.043 $\mu\text{mol s}^{-1}$ for $\text{Mn}_{1.1}\text{Co}_{1.9}\text{O}_4$ and 0.050 $\mu\text{mol s}^{-1}$ for Co_3O_4 .

Irradiation radius = 1 cm = 0.01 m

Photon flux: 0.522 $\mu\text{mol s}^{-1}$ ($\pi \times (0.01\text{m})^2 \times 1662 \mu\text{mol m}^{-2}\text{s}^{-1}$) for $\text{Fe}_{1.1}\text{Co}_{1.9}\text{O}_4$; ($\pi \times (0.01\text{m})^2 \times 1789 \mu\text{mol m}^{-2}\text{s}^{-1}$) for $\text{Mn}_{1.1}\text{Co}_{1.9}\text{O}_4$; ($\pi \times (0.01\text{m})^2 \times 1702 \mu\text{mol m}^{-2}\text{s}^{-1}$) for Co_3O_4 .

$$\Phi_{\text{AQY(initial)}} = 2 \times \frac{\text{initial Oxygen formation rate}}{\text{photon flux}} \times 100\%$$

, namely, 28.4% for $\text{Fe}_{1.1}\text{Co}_{1.9}\text{O}_4$; 15.3% for $\text{Mn}_{1.1}\text{Co}_{1.9}\text{O}_4$ and 18.7% for Co_3O_4 .

Mott-Schottky analysis

For p-type semiconductors, E_{fb} (flat-potential) values were calculated according to the below equation. Here, C_{SC}^{-2} and A are the interfacial capacitance and area, respectively. E_{app} is applied potentials, N_{D} the donor density, K is Boltzmann's constant, T the absolute

temperature, and q is the electronic charge, ϵ_0 the permittivity of free space, ϵ is the dielectric constant. KT/e is about 25 mV at room temperature and can be ignored.^{s2}

$$C_{SC}^{-2} = \frac{2 \left(-E_{app} + E_{fb} - \frac{KT}{q} \right)}{N_D \epsilon \epsilon_0 q A^2}$$

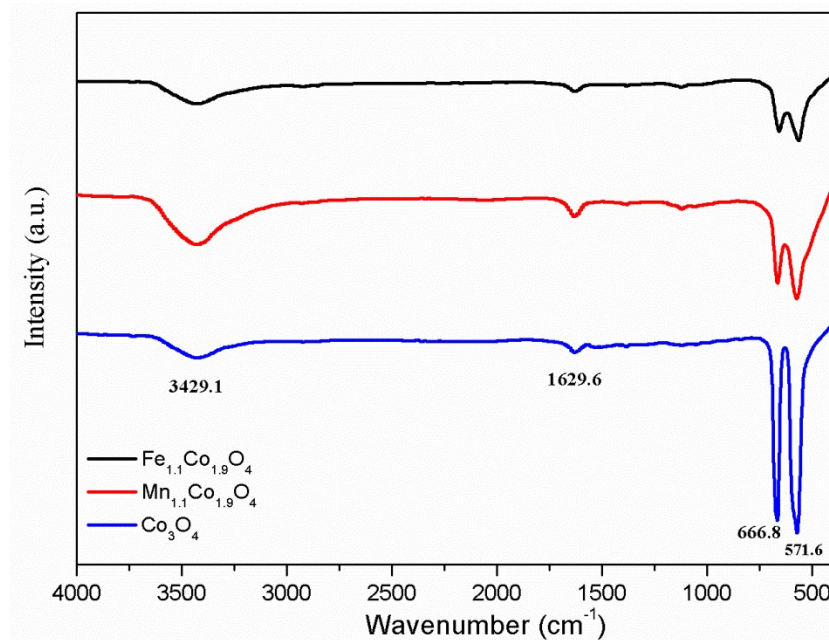


Figure S1. The FT-IR spectra of $M_{1.1}Co_{1.9}O_4$ samples.

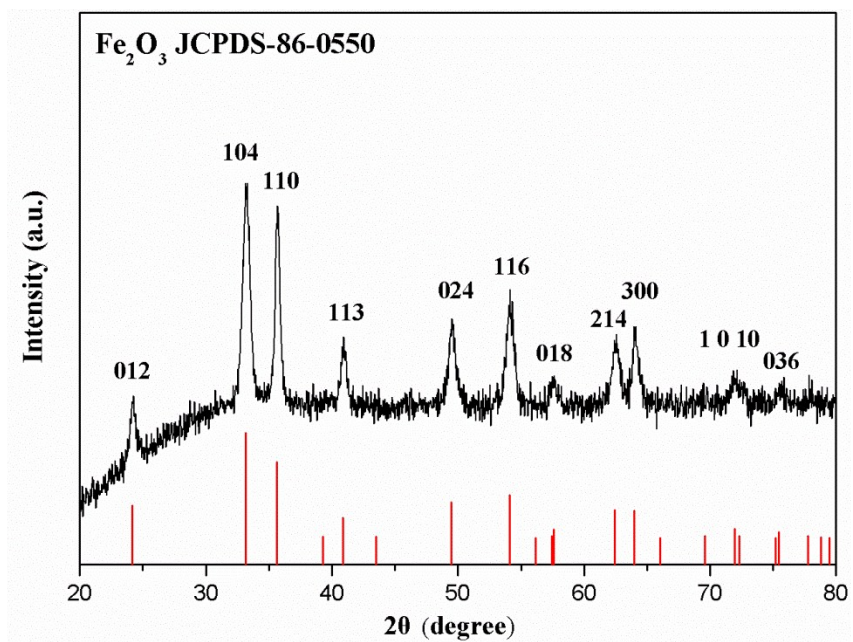


Figure S2. Powder XRD pattern of Fe₂O₃.

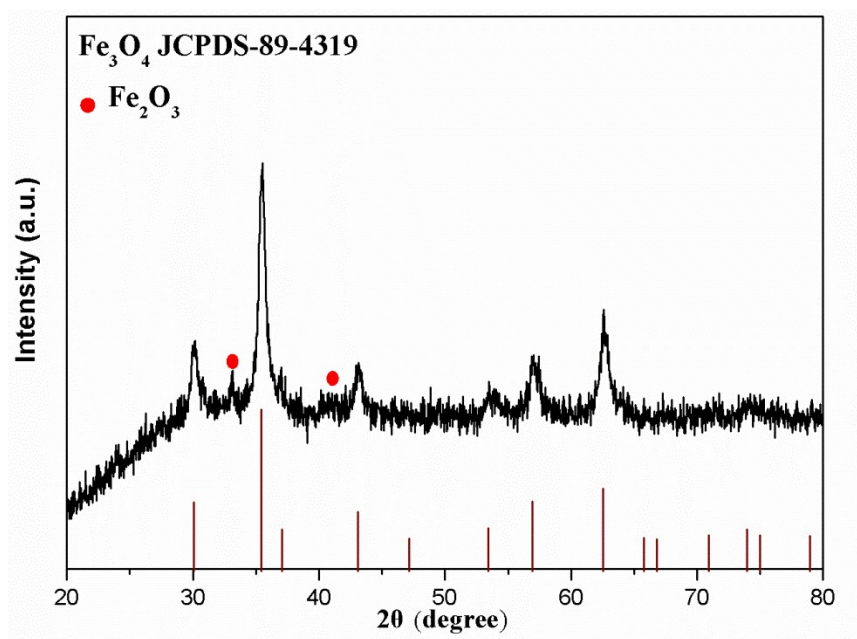


Figure S3. Powder XRD pattern of Fe₃O₄

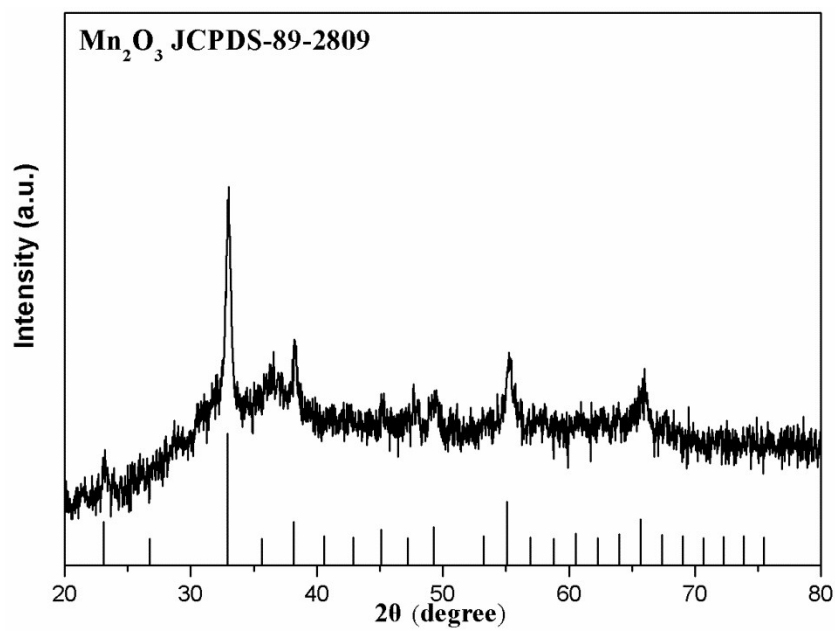


Figure S4. Powder XRD pattern of Mn₂O₃

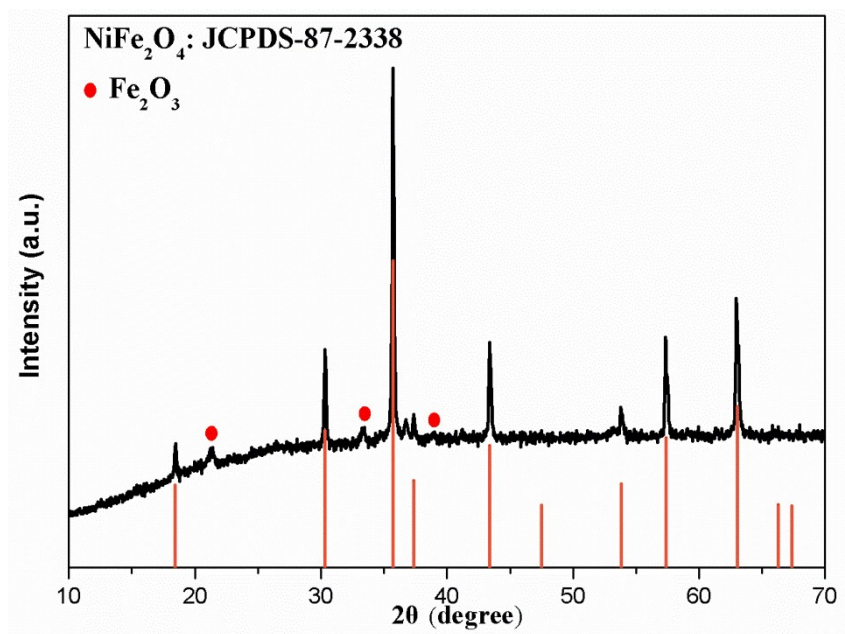


Figure S5. Powder XRD pattern of NiFe₂O₄

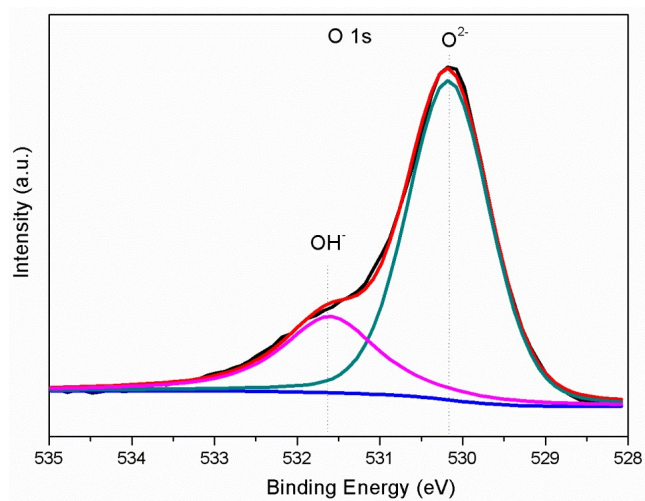


Figure S6. XPS of $\text{Fe}_{1.1}\text{Co}_{1.9}\text{O}_4$ sample in the O 1s energy region.

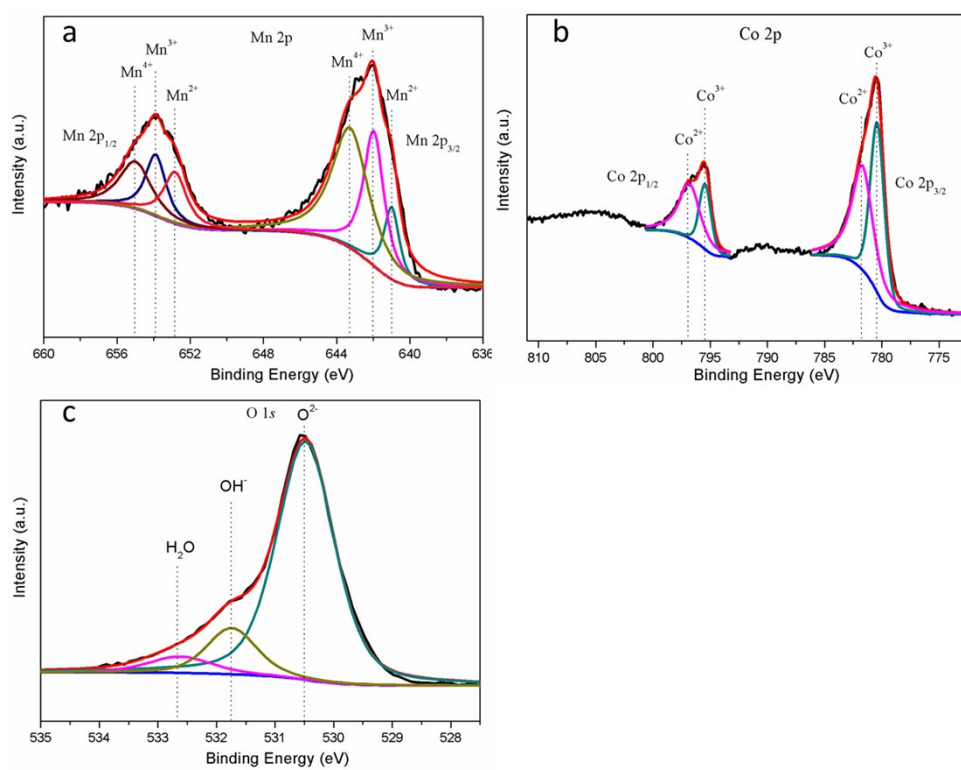


Figure S7. XPS of $\text{Mn}_{1.1}\text{Co}_{1.9}\text{O}_4$ sample.

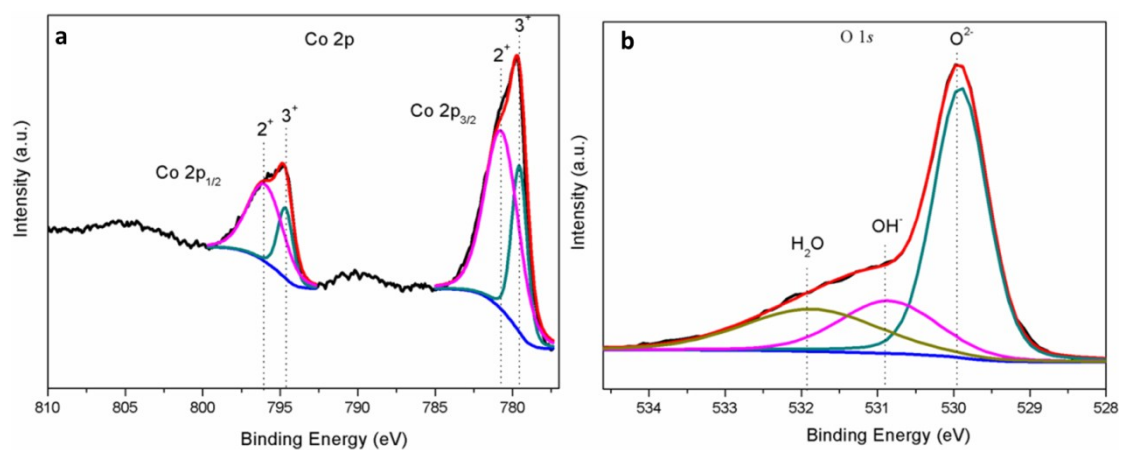


Figure S8. XPS of Co₃O₄ sample.

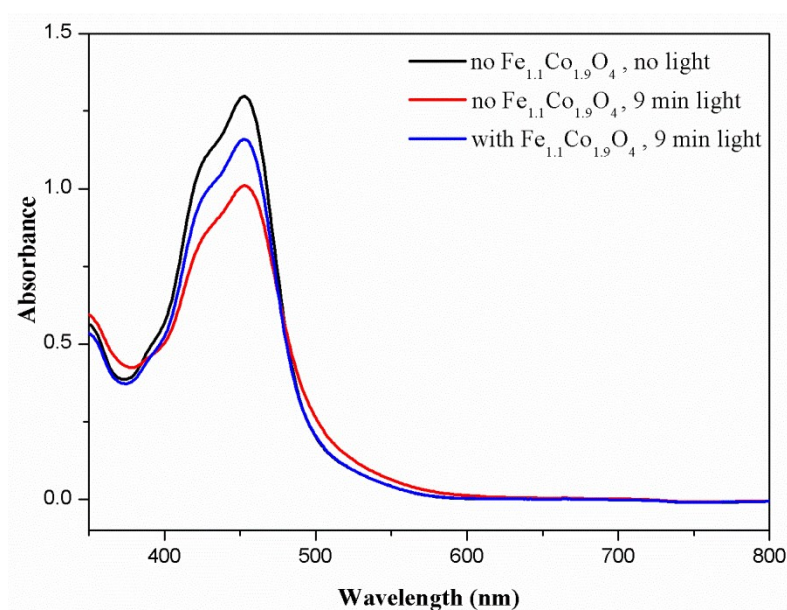


Figure S9. UV-vis spectral changes during the photocatalytic O₂ evolution ([Ru(bpy)₃]Cl₂-Na₂S₂O₈) with or without catalyst at pH 9.0. (Absorption of [Ru(bpy)₃]Cl₂ at 450 nm).

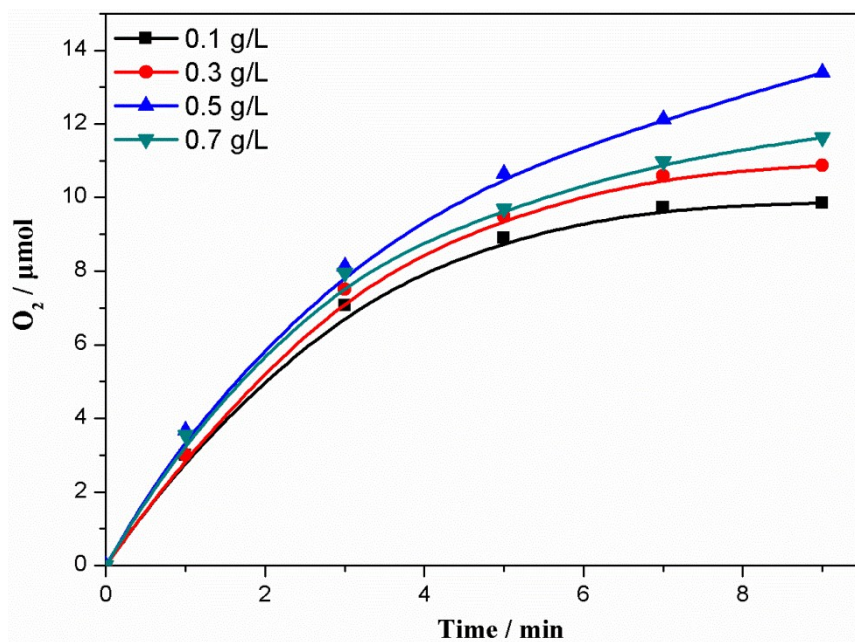


Figure S10. Time courses of O₂ evolution in the borate buffer solution (pH 8.5, 10.0 mL) containing Na₂S₂O₈ (5.0 mM), [Ru(bpy)₃]Cl₂ (1.0 mM) and Fe_{1.1}Co_{1.9}O₄ sample.

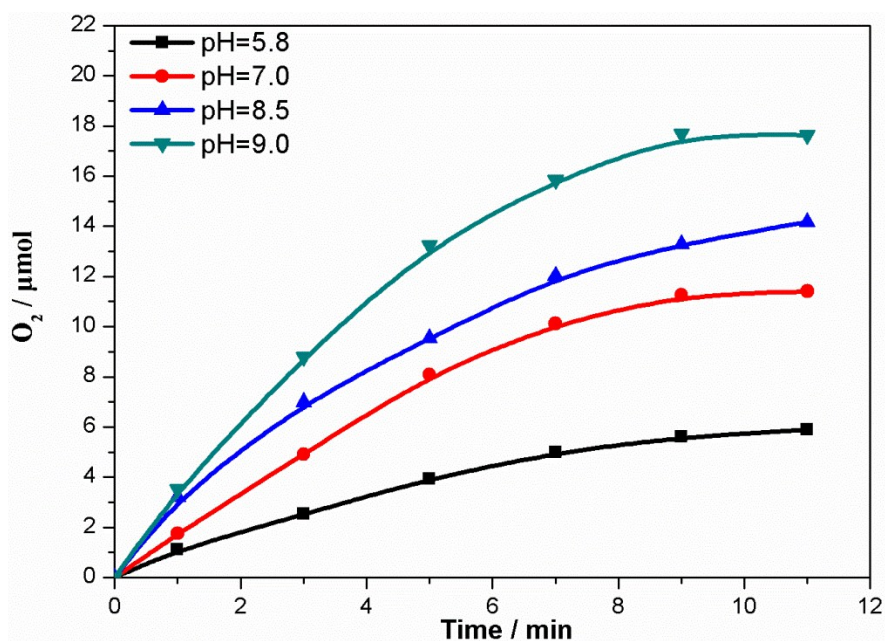


Figure S11. Time courses of O₂ evolution under photoirradiation containing Na₂S₂O₈ (5.0 mM), [Ru(bpy)₃]Cl₂ (1.0 mM), Fe_{1.1}Co_{1.9}O₄ (0.5 g L⁻¹).

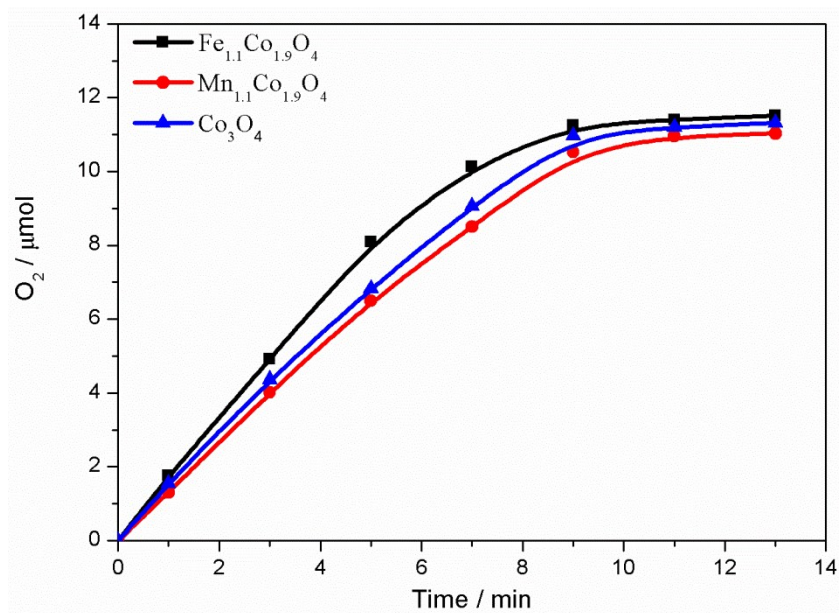


Figure S12. Time courses of O₂ evolution under photoirradiation in a phosphate buffer solution (pH 7.0, 10 ml) containing Na₂S₂O₈ (5.0 mM), [Ru(bpy)₃]Cl₂ (1.0 mM), Fe_{1.1}Co_{1.9}O₄ (0.5 g L⁻¹).

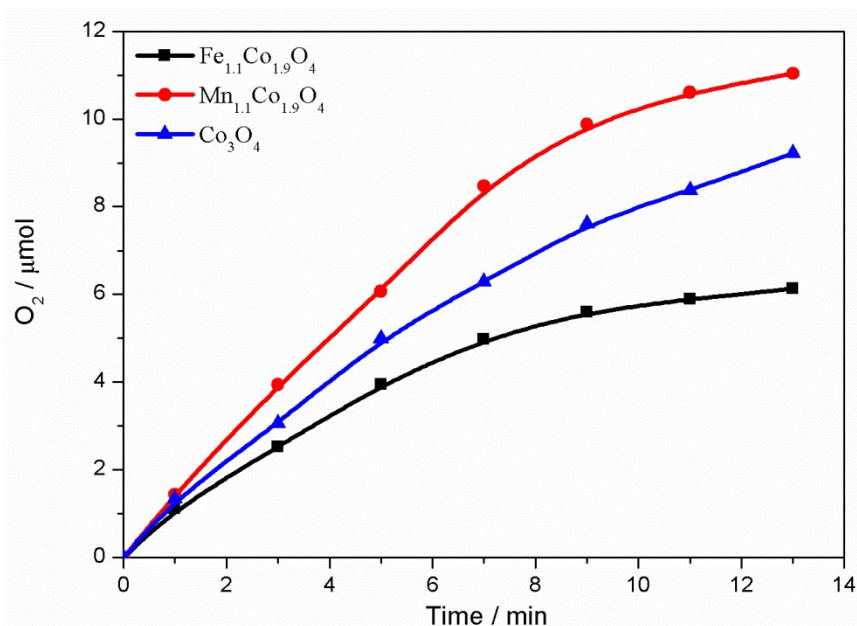


Figure S13. Time courses of O₂ evolution under photoirradiation in a Na₂SiF₆-NaHCO₃ buffer solution (pH 5.8, 10 ml) containing Na₂S₂O₈ (5.0 mM), [Ru(bpy)₃]Cl₂ (1.0 mM), Fe_{1.1}Co_{1.9}O₄ (0.5 g L⁻¹).

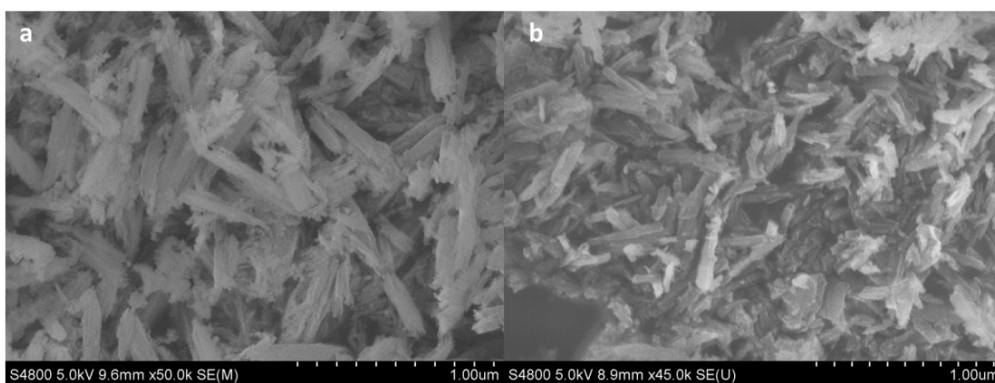


Figure S14. SEM images of fresh Fe_{1.1}Co_{1.9}O₄ sample (a) and recovered Fe_{1.1}Co_{1.9}O₄ sample (b).

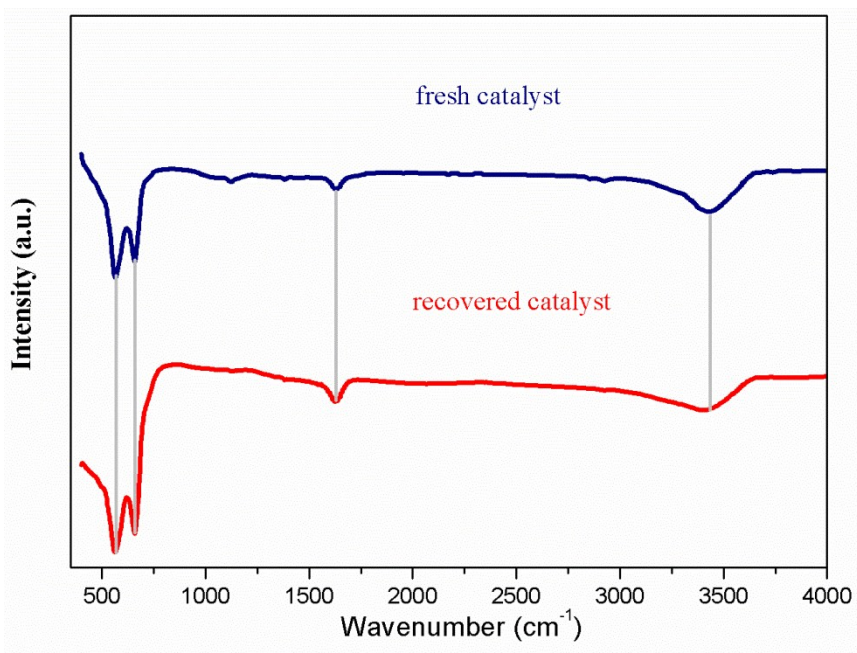


Figure S15. FT-IR spectra of fresh Fe_{1.1}Co_{1.9}O₄ sample (blue) and recovered Fe_{1.1}Co_{1.9}O₄ sample (red).

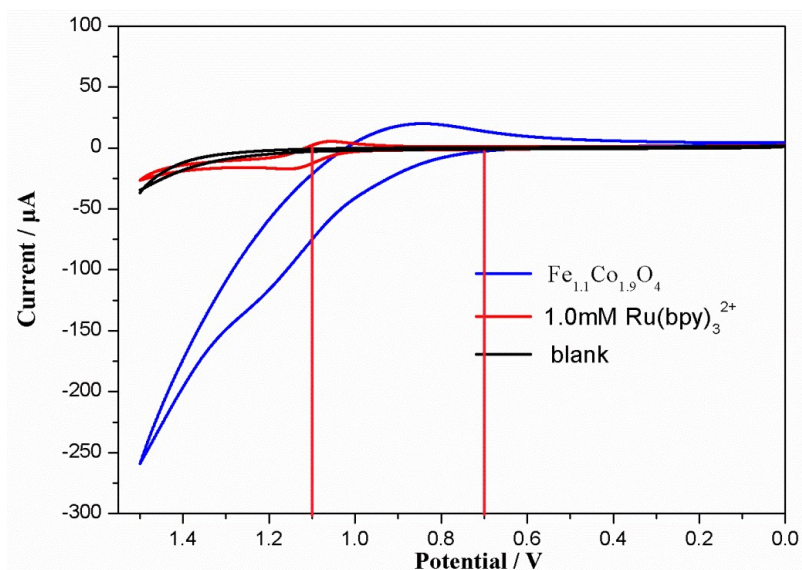


Figure S16. Cyclic voltammograms (CVs) of 80 mM sodium borate buffer solution at pH 9.0 with 1.0 mM $[\text{Ru}(\text{bpy})_3]\text{Cl}_2$ (red line) and $\text{Fe}_{1.1}\text{Co}_{1.9}\text{O}_4$ sample (blue line). The black line displays the CV of 80 mM sodium borate buffer solution (pH 9.0).

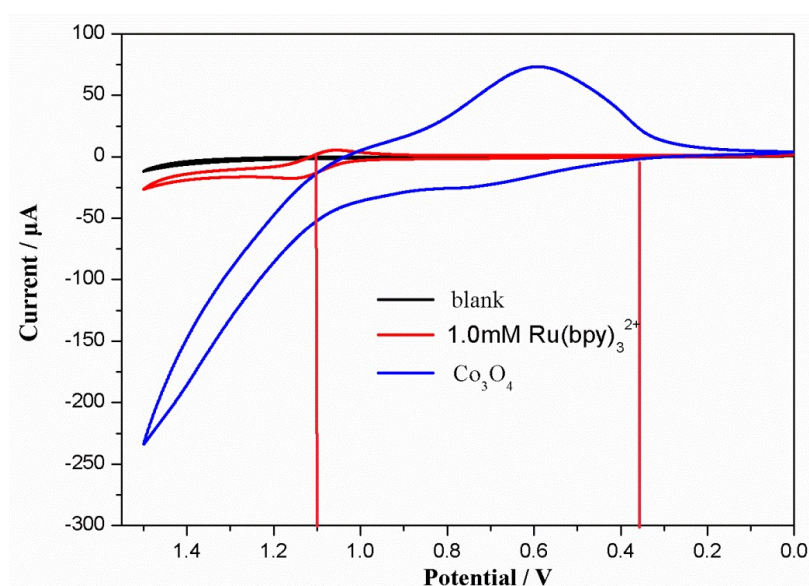


Figure S17. Cyclic voltammograms (CVs) of 80 mM sodium borate buffer solution at pH 9.0 with 1.0 mM $[\text{Ru}(\text{bpy})_3]\text{Cl}_2$ (red line) and Co_3O_4 sample (blue line). The black line displays the CV of 80 mM sodium borate buffer solution (pH 9.0). E (V) vs. Ag/AgCl.

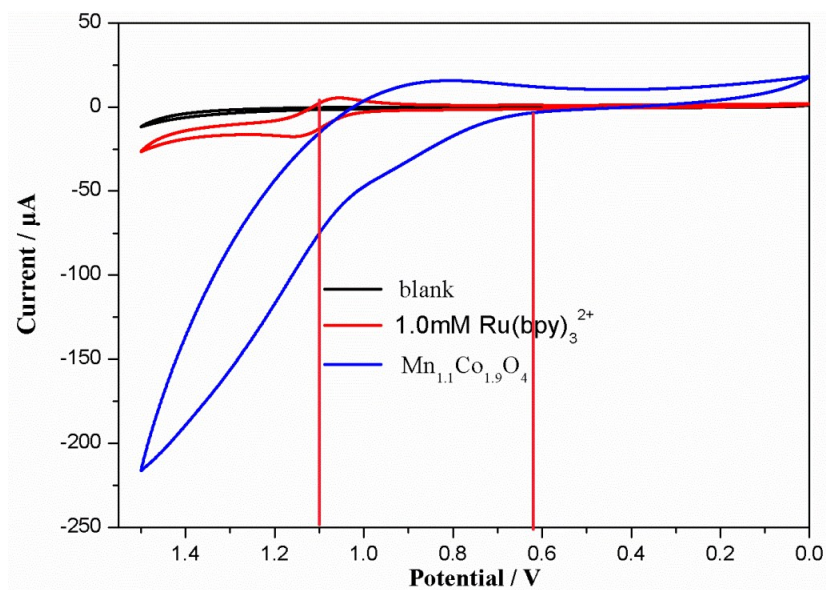


Figure S18. Cyclic voltammograms (CVs) of 80 mM sodium borate buffer solution at pH 9.0 with 1.0 mM [Ru(bpy)₃]Cl₂ (red line) and Mn_{1.1}Co_{1.9}O₄ sample (blue line). The black line displays the CV of 80 mM sodium borate buffer solution (pH 9.0). E (V) vs. Ag/AgCl.

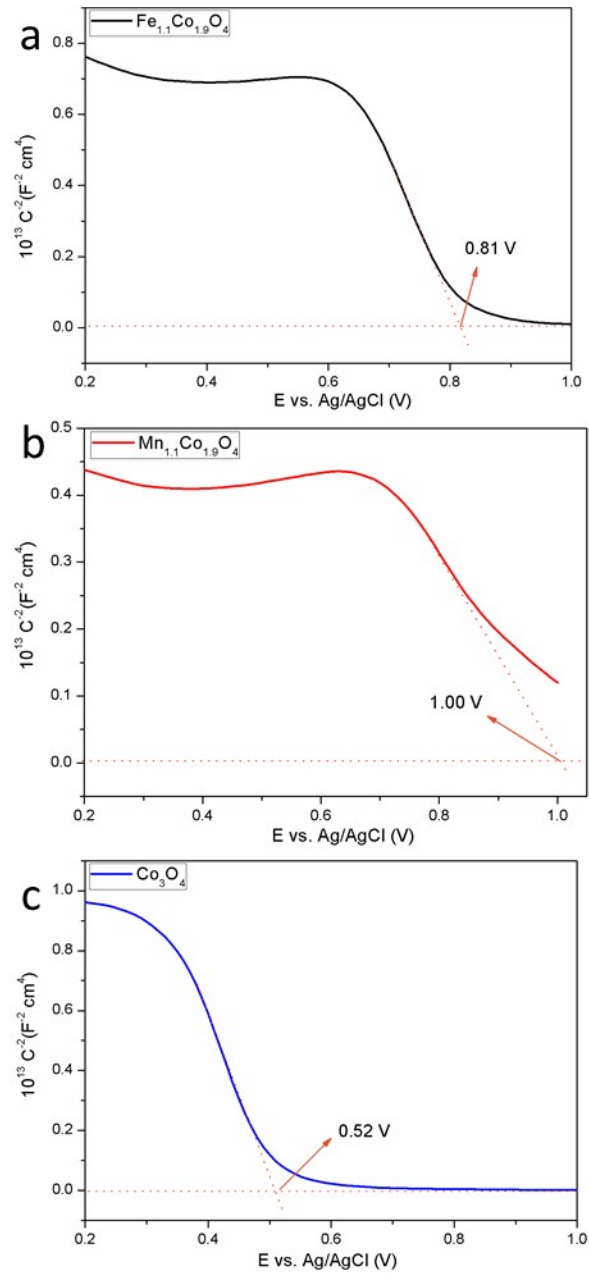


Figure S19. Mott-schottky plots and corresponding flat-band potential of (a) $\text{Fe}_{1.1}\text{Co}_{1.9}\text{O}_4$, (b) $\text{Mn}_{1.1}\text{Co}_{1.9}\text{O}_4$ and (c) Co_3O_4 .

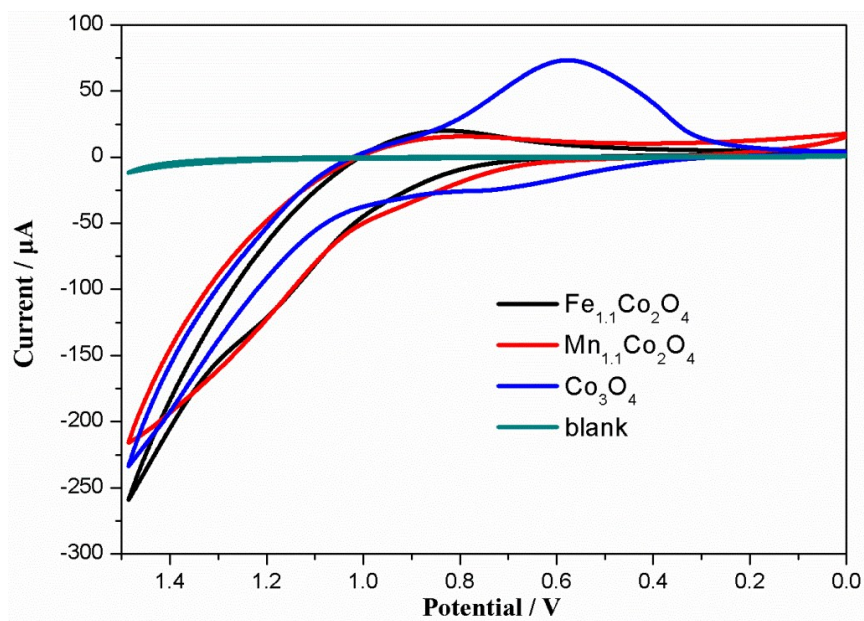


Figure S20. Cyclic voltammograms (CVs) of 80 mM sodium borate buffer solution at pH 9.0 with $M_nCo_{3-n}O_4$. The dark green line denotes the CV of 80 mM sodium borate buffer solution (pH 9.0). E (V) vs. Ag/AgCl.

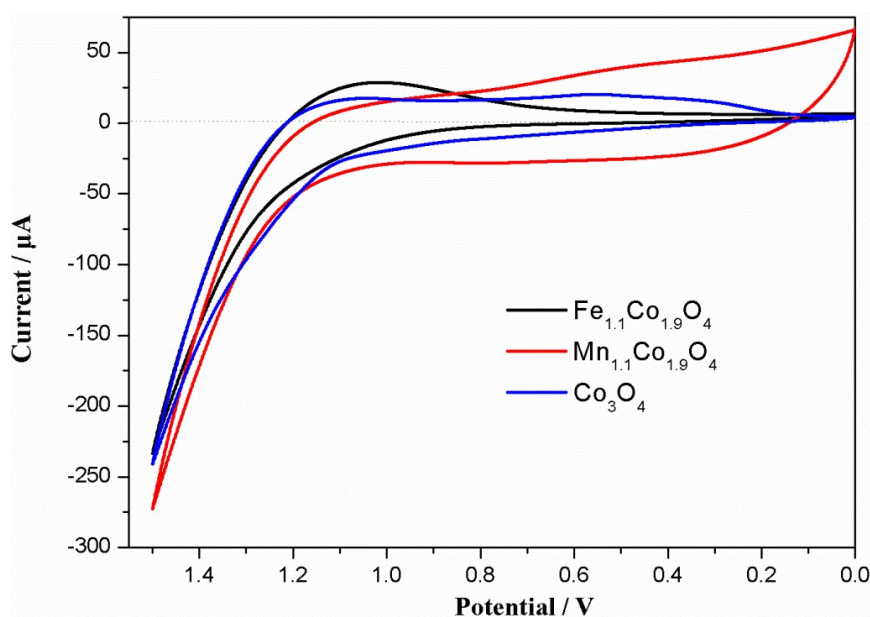


Figure S21. Cyclic voltammograms (CVs) of 20 mM $Na_2SiF_6-NaHCO_3$ buffer solution at pH 5.8 with $M_nCo_{3-n}O_4$. E (V) vs. Ag/AgCl.

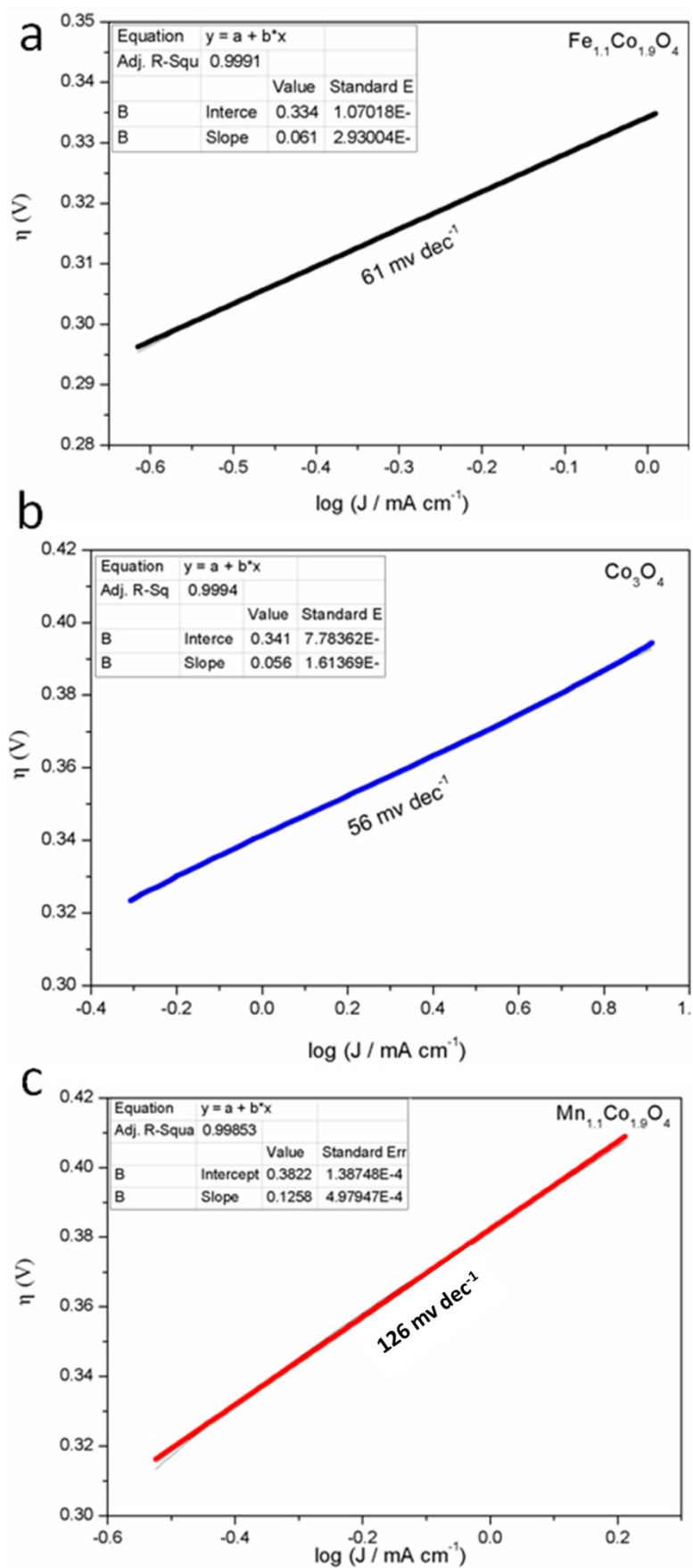


Figure S22. Tafel plots of $\text{M}_n\text{Co}_{3-n}\text{O}_4$ samples (a) $\text{Fe}_{1.1}\text{Co}_{1.9}\text{O}_4$; (b) Co_3O_4 ; (c) $\text{Mn}_{1.1}\text{Co}_{1.9}\text{O}_4$.

Table S1. Determination of metal elements ratio in as-prepared catalysts obtained by ICP-AES.

Catalysts	Estimated formula	Fe/Mn to Co ratio (ICP-AES)
$\text{Fe}_n\text{Co}_{3-n}\text{O}_4$	$\text{Fe}_{1.1}\text{Co}_{1.9}\text{O}_4$	1.16:2
$\text{Mn}_n\text{Co}_{3-n}\text{O}_4$	$\text{Mn}_{1.1}\text{Co}_{1.9}\text{O}_4$	1.18:2
Co_3O_4	Co_3O_4	N/A

Table S2. The photocatalytic activity of $\text{M}_n\text{Co}_{3-n}\text{O}_4$ samples for water oxidation. ^a

Catalysts	$\text{Fe}_{1.1}\text{Co}_{1.9}\text{O}_4$			$\text{Mn}_{1.1}\text{Co}_{1.9}\text{O}_4$			Co_3O_4		
pH	9.0	7.0	5.8	9.0	7.0	5.8	9.0	7.0	5.8
TOF _M (mmol mol _M ⁻¹ s ⁻¹)	0.93	0.47	0.30	0.65	0.31	0.38	0.85	0.41	0.36
R _{O2} (μmol s ⁻¹ g ⁻¹)	11.7	5.9	3.7	8.2	4.37	4.8	10.6	5.1	4.5
O ₂ yield (%)	71.0	46.0	24.5	45.3	44.1	44.2	52.6	42.9	36.9

^a Conditions: LED lamp (≥ 420 nm), 15.8 mW; 1.0 mM $[\text{Ru}(\text{bpy})_3]\text{Cl}_2$; 5.0 mM $\text{Na}_2\text{S}_2\text{O}_8$; 80 mM sodium borate buffer (pH=9.0), 100 mM sodium phosphate buffer (pH=7.0), 20 mM $\text{Na}_2\text{SiF}_6\text{-NaHCO}_3$ buffer (pH=5.8); total reaction volume, 10 mL; head space volume, 15 mL; and vigorous agitation using a magnetic stirrer.

Table S3. Oxygen yields of photocatalytic water oxidation among low-cost heterogenetic catalysts.

Catalysts	Representative reaction conditions	Oxygen yields (%)	Ref. ^a
$\text{Fe}_{1.1}\text{Co}_{1.9}\text{O}_4$	0.5g L ⁻¹ catalyst, 1.0 mM $[\text{Ru}(\text{bpy})_3](\text{ClO}_4)_2$, 5.0 mM $\text{Na}_2\text{S}_2\text{O}_8$, 80 mM sodium borate buffer (pH 9.0)	90.4	This work
$\text{Mn}_{1.1}\text{Co}_{1.9}\text{O}_4$	0.5g L ⁻¹ catalyst, 1.0 mM $[\text{Ru}(\text{bpy})_3](\text{ClO}_4)_2$, 5.0 mM $\text{Na}_2\text{S}_2\text{O}_8$, 80 mM sodium borate buffer (pH 9.0)	59.2	This work
Co_3O_4	0.5g L ⁻¹ catalyst, 1.0 mM $[\text{Ru}(\text{bpy})_3](\text{ClO}_4)_2$, 5.0 mM $\text{Na}_2\text{S}_2\text{O}_8$, 80 mM sodium borate buffer (pH 9.0)	68.8	This work
NiFe_2O_4	0.5g L ⁻¹ catalyst, 1.0 mM $[\text{Ru}(\text{bpy})_3](\text{ClO}_4)_2$, 5.0 mM $\text{Na}_2\text{S}_2\text{O}_8$, 80 mM sodium borate buffer (pH 9.0)	85.9	This work

Fe ₂ O ₃	0.5g L ⁻¹ catalyst, 1.0 mM [Ru(bpy) ₃]Cl ₂ , 5.0 mM Na ₂ S ₂ O ₈ , 80 mM sodium borate buffer (pH 9.0)	20.4	This work
Mn ₂ O ₃	0.5g L ⁻¹ catalyst, 1.0 mM [Ru(bpy) ₃]Cl ₂ , 5.0 mM Na ₂ S ₂ O ₈ , 80 mM sodium borate buffer (pH 9.0)	36.0	This work
Fe ₃ O ₄	0.5g L ⁻¹ catalyst, 1.0 mM [Ru(bpy) ₃]Cl ₂ , 5.0 mM Na ₂ S ₂ O ₈ , 80 mM sodium borate buffer (pH 9.0)	39.3	This work
NiFe ₂ O ₄	0.5g L ⁻¹ catalyst, 0.25 mM [Ru(bpy) ₃]Cl ₂ , 5.0 mM Na ₂ S ₂ O ₈ , 50 mM phosphate buffe (pH 8.0)	74.0	22 ^a
CuFe ₂ O ₄	0.5g L ⁻¹ catalyst, 1.0 mM [Ru(bpy) ₃]Cl ₂ , 5.0 mM Na ₂ S ₂ O ₈ , 80 mM sodium borate buffer (pH 8.5)	72.8	46 ^a
LaCoO ₃	0.25g L ⁻¹ catalyst, 0.25 mM [Ru(bpy) ₃]Cl ₂ , 5.0 mM Na ₂ S ₂ O ₈ , 50 mM phosphate buffe (pH 8.0)	74.0	45 ^a

^a see as the main text references.

Table S4. Flat-band potentials of M_nCo_{3-n}O₄ samples.

Catalysts	Flat-band potential (V vs. Ag/AgCl)	Flat-band potential (V vs. NHE)
Fe _{1.1} Co _{1.9} O ₄	0.81	1.02
Mn _{1.1} Co _{1.9} O ₄	1.00	1.21
Co ₃ O ₄	0.52	0.73

REFERENCES

- S1. Wang, L.; Li, J.; Jiang, Q.; Zhao, L., *Dalton Trans.* **2012**, *41*, 4544-4551.
 S2. Fabregat-Santiago, F.; Garcia-Belmonte, G.; Bisquert, J.; Bogdanoff, P.; Zaban, A., *J. Electrochem. Soc.* **2003**, *150*, E293-E298.